ELSEVIER

Catalysis Today 43 (1998) 123–133

CATALYSIS TODAY

Relationship between hydrodesulfurization activity and morphological and structural changes in NiW hydrotreating catalysts supported on Al_2O_3–TiO_2 mixed oxides

Jorge Ramírez*, Aída Gutiérrez-Alejandre

UNICAT, Depto. de Ingeniería Química, Facultad de Química, UNAM, Cd. Universitaria, Mexico D.F. (04510), Mexico

Abstract

Characterization and catalytic activity of the NiW-based catalysts supported on Al–Ti(x) mixed oxides has been obtained. The results from the characterization techniques (Surface area, XRD, DRS, TPR, XPS, FTIR of adsorbed NO and HREM) were used to establish a relationship between the morphological and structural changes of the tungsten phases and catalytic activity. The results indicate that the incorporation of titania to the support enhances the reducibility and sulfidability of the tungsten phases due to mainly a reduced interaction of the tungsten phases with the support. Correlation of the catalytic activity in the thiophene HDS reaction and the number of tungsten atoms in edge and corner positions in the WS_2 crystallites indicates that only the number of tungsten atoms equivalent to those present in one layer of the WS_2 crystallites are active at a given time.

Keywords: NiW; Hydrodesulfurization catalysts; Al_2O_3–TiO_2 mixed oxides; Activity; Characterization

1. Introduction

In the search for better hydrotreating catalysts, it has been found that the nature of the support plays an important role to improve the HDS activity. For example, it has been found that the titania supported CoMo catalysts have 1.9 times the HDS activity of their alumina supported counterparts [1]. However, since the titania polymorph, anatase, shows low-thermal stability and -surface area, some other alternatives must be used. Among these, the use of titania–alumina mixed oxides has been proposed as an interesting alternative [2]. Also, in the case of W-based catalysts, the use of alumina as support leads to a strong interaction between the tungsten oxidic phases and the alumina support, which diminishes the degree of sulfidation of the former ones [3,4]. To overcome this problem, in a previous work, we studied the effects that the change in the nature of the support produced in the state of the W oxidic supported phases as the nature of the support changed from alumina to titania [5]. The results from this study showed that W catalysts supported on titania-rich Al_2O_3–TiO_2 mixed oxide supports have a greater HDS activity than those supported on alumina and that it is possible to obtain catalysts with higher surface areas than TiO_2 even for Al_2O_3–TiO_2 mixed oxides with 95% mol content of TiO_2. Also, good dispersion and reducibility of the W oxidic

*Corresponding author. Fax: (525)6225366; e-mail: jrs@servidor.unam.mx

0920-5861/98/$32.00
PII S0920-5861(98)00141-2

phases was obtained by the incorporation of titania to the alumina support.

It is well known that the presence of the Ni promoter also improves the reducibility and dispersion of the W phases. Therefore, it seems interesting to study the behavior of Ni-promoted W based catalysts supported on Al–Ti(x) mixed oxides to benefit from both, the Ni promotion and the presence of TiO_2 in the support, which leads to higher HDS activities. To this end, a series of W and NiW/Al_2O_3–TiO_2 catalysts with different support compositions were prepared and characterized in their oxided and sulfided forms. The results from these characterizations will be used to estimate the changes in the degree of reducibility (TPR), dispersion (XPS, FTIR of adsorbed NO) and catalyst sulfidation (HREM) with the titanium content and to build a geometrical model of the sulfided catalysts to explain the catalytic activity changes for the thiophene hydrodesulfurization reaction, in terms of the architectural changes of the WS_2 crystallites.

2. Experimental

2.1. Supports and catalysts preparation

A series of nickel–tungsten catalysts supported on alumina–titania mixed oxides with a molar ratio $x=TiO_2/(Al_2O_3+TiO_2)=0$, 0.1, 0.5, 0.7, 0.95 and 1.0 have been prepared. The supports were prepared by the co-precipitation of the required amounts of aluminum (AIP) and titanium (TIP) isopropoxides following the same method described previously [5]. In short, after the dissolution of AIP in n-propanol, under vigorous stirring the required amount of TIP was added. The hydrolysis of the alkoxides was achieved by adding an amount of demineralized water equal to 33 times the stoichiometric amount. The precipitate was maintained for 24 h under slow agitation and then filtered and washed with water, dried at 373 K during 24 h and calcined at 773 K for 24 h. Hereafter, the supports will be named Al–Ti(x), where x is equal to the molar ratio $TiO_2/(TiO_2+Al_2O_3)$.

The unpromoted catalysts were prepared with a metal loading of 2.8 atoms of W per square nanometer of support surface by impregnating the supports with an aqueous solution of ammonium metatungstate ($(NH_4)_6H_2W_{12}O_{40}$). After impregnation, the catalysts were dried at 373 K for 18 h and calcined for 3 h at 773 K. With respect to the promoted catalysts, they were prepared using an atomic ratio of $Ni/(Ni+W)=0.3$ by successive impregnation of the tungsten-based catalysts with an aqueous solution of nickel nitrate ($Ni(NO_3)_2\cdot 6H_2O$) which contained the required amount of nickel. The impregnated samples were then dried and calcined at similar conditions as the unpromoted catalysts. The catalysts will be referred as NiW/Al–Ti(x).

2.2. Supports and oxidic catalysts characterization

The specific surface areas of the catalyst samples were determined by nitrogen physisorption using a Pulse Chemisorb 2700 Micromeritics apparatus. The X-ray diffraction (XRD) patterns were obtained in a Siemens D-500 diffractometer, using the CuKα radiation ($\lambda=1.5418$). The diffuse reflectance UV–VIS spectra (DRS), were taken in a Cary |5E| UV–VIS–NIR spectrometer, using the supports as reference. Temperature programmed reduction (TPR) measurements were recorded in a flow apparatus following the procedure reported previously [5]. X-ray photoelectron spectroscopy (XPS) analysis was performed in a Perkin-Elmer spectrometer using monochromatic Al Kα radiation. The C1s binding energy of spurious carbon (BE=284.5 eV) was taken as reference.

2.3. Sulfided catalysts characterization

The sulfidation of the catalysts' oxidic precursors were carried out in the same reactor, before the activity was measured, with an H_2/H_2S 15% (v/v) gas mixture for 4 h at 673 K. The high resolution electron microscopy (HREM) micrographs were recorded in a Jeol 2010 microscope with a 0.17 nm resolution. With respect to the Fourier transform infrared (FTIR) experiments using NO as probe molecule, they were performed using a Nicolet 510 model FTIR spectrometer with a resolution of 4 cm^{-1} and 500 scans and a high vacuum glass cell connected to a gas manipulation manifold. The wafers of the oxidic powders were sulfided in the glass cell using the same conditions as above. After sulfidation and evacuation, 40 torr of NO gas were introduced to the IR cell and the spectra recorded.

2.4. Catalytic activity

The catalytic activity test were conducted in a typical microreactor apparatus. Hydrogen was bubbled through a saturator filled with thiophene, maintained at 273 K. The gas mixture was passed through a heated Pyrex reactor with temperature regulation, operating at atmospheric pressure, which contained 0.1 g of catalyst. Reactant and products analysis were performed by on-line gas chromatography. All of the catalytic activities reported here are steady-state values reached after the catalyst had been stabilized during 12 h. Activity measurements were obtained at 563 K and the experiments were performed at low conversions, below 15%.

3. Results

3.1. Catalytic activity

The results from the catalytic activity of the NiW/Al–Ti(x) catalysts are presented in Fig. 1. To allow a good comparison of the catalysts, since they have widely different surface areas, the rates of hydrodesulfurization have been normalized by the total amount of W atoms and are therefore expressed as molecules of thiophene converted per second and per atom of W impregnated on the catalyst. It is clear from the results in Fig. 1 that high titania contents in the catalyst ($x \geq 0.7$) lead to a substantial increase in the HDS activity. In contrast, at low titanium contents ($x \leq 0.5$) the catalyst activity resembles that of the pure alumina supported catalyst. In fact, for the Ni-promoted catalysts with a ratio of x=0.7, 0.95 and 1.0 at 563 K, the HDS activity with respect to the pure alumina supported catalyst increases 1.15, 2.22, and 4.16 times, respectively.

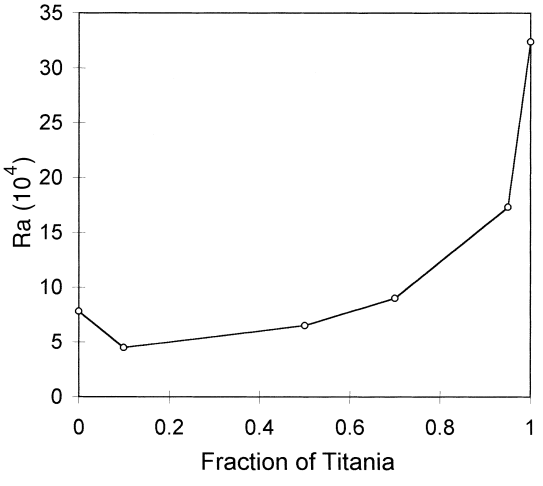

Fig. 1. Activity results of NiW/Al–Ti(x) catalysts at T=563 K; Ra=Thiophene molecules/W atom-s: Fraction of Titania=(TiO_2/(TiO_2+Al_2O_3)).

The origin of these substantial activity increases must lie, at least in part, in the dispersion, morphological and structural changes of the W and Ni phases induced by the support formulation. The electronic effects produced on the tungsten phases by the presence of TiO_2 in the catalyst are beyond the objective of the present work and will be addressed in future publications.

3.2. Catalyst characterization

The compositions and surface areas of the different catalysts are presented in Table 1. It is observed that up to support compositions corresponding to x=0.5, the surface area is maintained at values close to those of the pure alumina supported catalyst. At values of $x \geq 0.7$, the surface area decreases and the pure titania supported sample shows an area of only 10 m^2/g. However, incorporation of 5% Al_2O_3 in the Al_2O_3–TiO_2 mixed oxide preserves areas of 61 m^2/g giving an indication that alumina is a textural promoter for TiO_2.

The results from XRD give no indication, at this scale of measuring, of the presence of WO_3 or NiO crystallites in any of the samples, indicating therefore a good dispersion of the tungsten and nickel phases. In fact, the catalysts' diffractograms are quite similar to those of the corresponding supports.

Table 1
Molar TiO_2/TiO_2+Al_2O_3 ratios (x) and surface areas (S_g) of the different NiW/Al–Ti(x) catalysts

Catalysts	x	S_g (m^2/g)
NiW/Al–Ti(0)	0.00	157
NiW/Al–Ti(0.1)	0.10	188
NiW/Al–Ti(0.5)	0.50	186
NiW/Al–Ti(0.7)	0.70	144
NiW/Al–Ti(0.95)	0.95	61
NiW/Al–Ti(1.0)	1.0	10

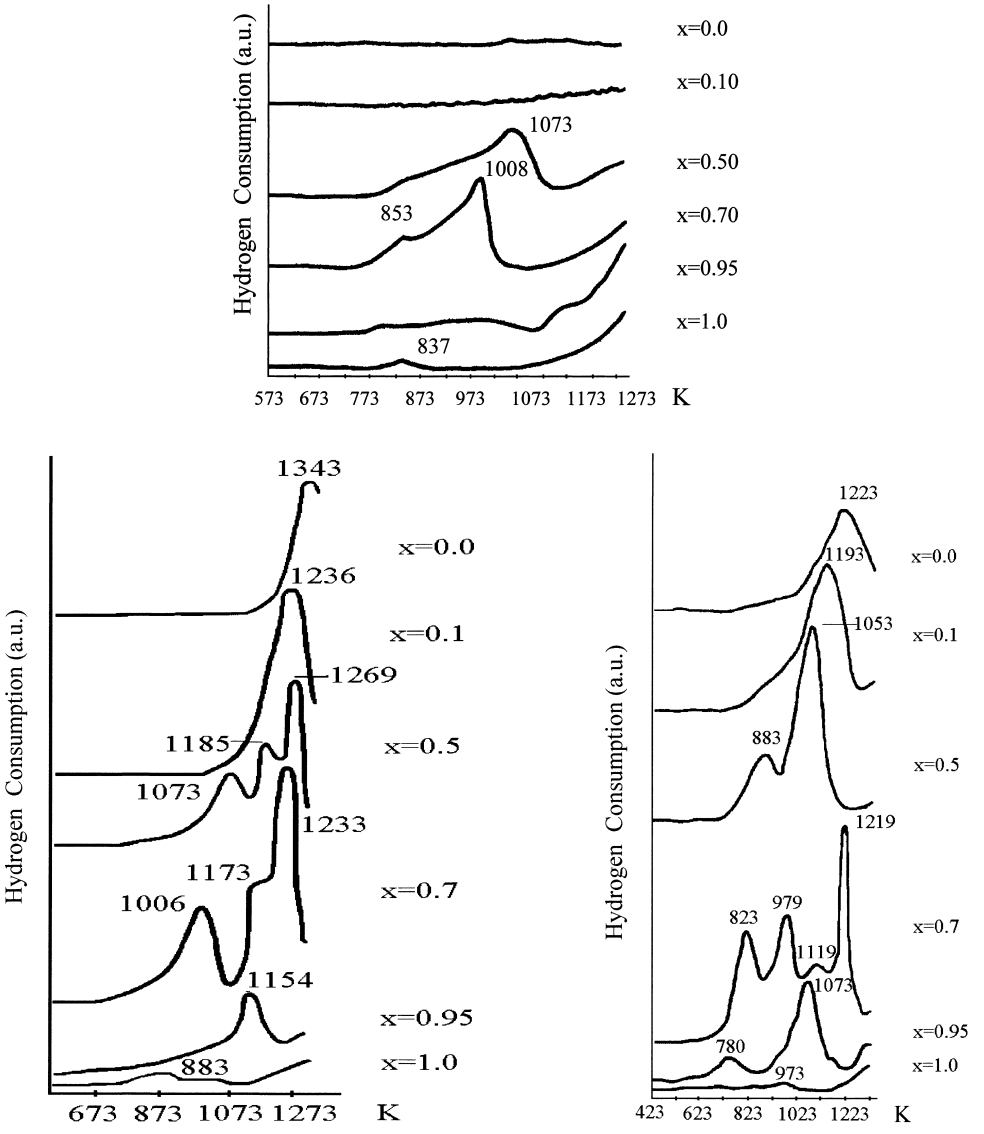

Fig. 2. TPR patterns of (a) Al–Ti(x) supports; (b) W/Al–Ti(x) oxidic catalysts and (c) NiW/Al–Ti(x) oxidic catalysts.

Fig. 2(a)–(c) shows the TPR patterns of supports, unpromoted and promoted catalysts, respectively. Due to the complexity of the NiW/Al–Ti(x) TPR patterns it will be necessary for its interpretation to compare them with those of the supports and of the unpromoted W/Al–Ti(x) samples. A previous discussion about supports and unpromoted catalysts has been given elsewhere [5], we will therefore concentrate here on the promoted system.

The NiW catalyst supported on pure alumina shows, in agreement with the unpromoted system and with previous results [5–7], a single high temperature reduction peak. However, this peak is broader than that of the unpromoted catalyst and presents the maximum at T_{max}=1223 K, which is about 120 K lower than for the unpromoted catalyst. Since in this sample the alumina support does not undergo reduction, it appears clearly that the presence of Ni in the

catalyst promotes the reduction of the tungsten species at lower temperature. Although the reduction peaks of Ni species are not clearly evident in this sample they may contribute to the broadness of the observed peak. According to the previous works [6], the Ni species show peaks of reduction at 600 K (NiO), 960 K ($NiWO_4$) and 1220 K and a shoulder at 1030 K. ($NiAl_2O_4$).

As titanium is incorporated into the support the high temperature reduction peak shifts to lower temperatures and a shoulder which in the NiW/Al–Ti(0.1) sample appears at 923 K develops into a clear peak (T_{max}=883 K) in the NiW/Al–Ti(0.5) sample. This low temperature peak was assigned, by comparison with the corresponding pure support pattern, to the reduction of TiO_2, anatase.

The NiW/Al–Ti(0.7) sample presents a more complex TPR pattern with the presence of four reduction peaks at 823, 979, 1119 and 1219 K. The peak at 823 K is assigned to the reduction of anatase, the peak at 979 K might be due to the first stage of reduction of $W^{6+} \rightarrow W^{4+}$, which has been reported to occur at T_{max}=1017 K in W/TiO_2 [7].

The peak at 1119 K could possibly be due to the second stage of reduction $W^{4+} \rightarrow W^0$ reported previously at T_{max}=1248 K for W catalysts supported on titania [7]. The appearance of this second stage of W reduction is due to the stabilization of the W^{4+} oxidation state by the titania. The high temperature reduction peak at 1219 K seems to be due to either the reduction of some W or Ni species which become loose as the surface area of the TiO_2, anatase, collapses into the rutile phase since the NiW/Al–Ti(0.7) sample had originally a surface area greater than 150 m^2/g. However, it has been found previously [8] that the incorporation of tungsten to anatase stabilizes its structure and the phase transformation to rutile occurs at 1270 K rather at 970 K. It would be then improbable that the reduction peak be due to W or Ni species which become lose during the surface area collapse of the anatase when transforming into rutile.

The titanium rich samples do not lend themselves to clear interpretation due to the low amount of tungsten present in them which results from the low surface areas of these samples. With respect to the XPS characterization, previous literature reports [3,9,10] indicate that bindings energies for the $W4f^{7/2}$ is 35.3 eV and 35.5–36.4 eV for tungsten in $NiWO_4$ and WO_3, respectively. According to this, in our samples where a small shift is observed from 35.57 to 36.14 eV as the titanium content varied from x=0 to x=1, it appears that no $NiWO_4$ exists in the titanium rich catalysts (x=0.95, 1.0). We believe that no $Al_2(WO_4)_3$ is present in the catalysts since the BE of the O*1s* level in this compound has been reported at 531.1–531.8 eV [9], whereas the experimental values found here are 529.99±0.14 eV.

The BE values of the Al*2p* level in the catalyst samples are typical of those reported for γ-Al_2O_3, BE=74.5 eV [11] with the exception of the NiW/Al–Ti(0.1) sample (BE=73.7 eV) in which some $NiAl_2O_4$, BE=73.8–74.0 eV [9,10] might be present.

The BE of the $Ti2p^{3/2}$ also shows a small shift towards higher BE's with titanium content from 457.84 eV in the NiW/Al–Ti(0.1) catalyst to 458.67 eV in the NiW/Al–Ti(1.0) catalyst. The difference with the reported value for TiO_2 samples, BE=458.5 eV [11], might be due to the formation of Al–O–Ti links as the aluminum content in the catalyst increases.

The atomic concentrations calculated from the XPS spectra of the different catalysts are presented in Table 2. Here, Ni reaches a maximum concentration in the NiW/Al–Ti(0.5) catalyst. However, one must be

Table 2
Atomic concentrations calculated from the XPS spectra of the different NiW/Al–Ti(x) catalysts; x=TiO_2/(TiO_2+Al_2O_3)

Catalyst	$Ni2p^{3/2}$	$W4f^{7/2}$	$Ti2p^{3/2}$	O*1s*	Al*2p*
NiW/Al–Ti(0)	35.40	244.63	–	3760.86	5899.99
NiW/Al–Ti(0.1)	55.79	498.50	382.26	4739.11	7646.35
NiW/Al–Ti(0.5)	66.85	530.83	1682.71	3946.61	4062.71
NiW/Al–Ti(0.7)	59.27	521.96	1646.04	2992.40	1959.85
NiW/Al–Ti(0.95)	48.06	691.44	3765.99	4366.12	1033.25
NiW/Al–Ti(1.0)	49.69	323.46	2266.40	2518.29	–

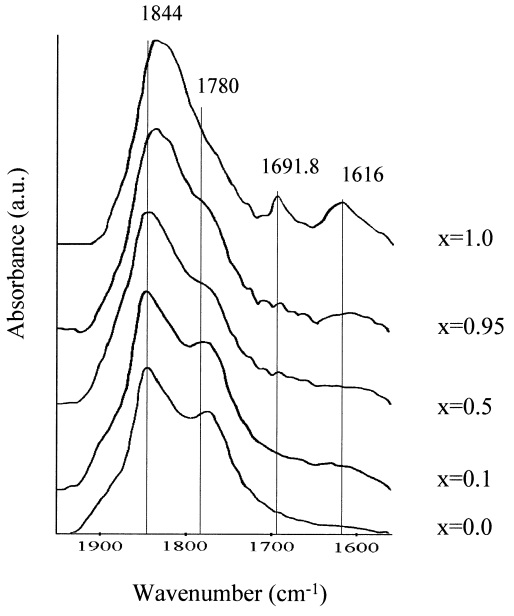

Fig. 3. NO adsorption FTIR spectra of NiW/Al–Ti(x) sulfided catalysts.

aware of the possibility of several species of each element contributing to the XPS signal i.e. NiO and $NiAl_2O_4$, and therefore not all of them may be precursors of the active phase. In contrast, W shows a maximum in the NiW/Al–Ti(0.95) catalyst, indicating that not all the Ni on the surface is contributing to the promotion of W.

The spectra of chemisorbed NO on the different sulfided NiW/Al–Ti(x) catalysts are presented in Fig. 3. For the NiW/Al–Ti(0) catalyst, it is possible to observe two well defined bands at ~1844 and ~1780 cm^{-1} and the presence of a shoulder at about 1887 cm^{-1}. The band at 1844 cm^{-1} was assigned in agreement with previous reports [12–14], to adsorbed NO on sulfided Ni^{2+} species. The spectra of all the catalyst samples show this band, however, in the rich-titania samples the band shifts 9 cm^{-1} to lower frequencies, indicating a more complete sulfidation of the Ni species. The band at 1780 cm^{-1} has been assigned to adsorbed NO on sulfided W^{4+} species. This assignment is in good agreement with previous literature reports [14]. Under evacuation at room temperature, this band disappears indicating a very weak adsorption of NO on sulfided W species. As titanium is incorporated into the support this band becomes less defined due to the overlap which occurs with the band of adsorbed NO on Ni species while the latter increases in intensity and shifts to lower frequencies. In fact, in the NiW/Al–Ti(1.0) catalyst it is only possible to see a single broad band with maximum at 1832 cm^{-1} which encompasses the contributions of adsorbed NO on sulfided Ni^{2+} and W^{4+} (see Fig. 3). Also, the presence of two bands in the 1600–1700 cm^{-1} region becomes more evident as the content of titanium in the support increases. These bands, which are quite clear in the NiW/Al–Ti(1.0) sample, have been assigned to contributions of adsorbed NO on sulfided titanium species. This assignment was corroborated by independent experiments which showed the presence of these two bands when NO was adsorbed on pure TiO_2 samples sulfided under the same conditions as the NiW/Al–Ti(x) catalysts.

Finally, the high frequency shoulder, which in the NiW/Al–Ti(0) sample appeared at about 1900 cm^{-1}, and which became less evident as the titanium content increased, was assigned according to previous reports [12,13] to adsorbed NO on Ni^{2+} species on oxidic surroundings. Deconvolution of the peaks in the different catalysts′ spectra showed that the shoulder was due to the presence of a small band at frequencies between 1860 and 1887 cm^{-1} which, in agreement with the previous observations, diminished with the titanium content and disappeared completely in the NiW/Al–Ti(1.0) catalyst sample. Quantification of the above adsorbed NO results was made by normalizing the peak areas per square meter of catalyst. These results show that the band of adsorbed NO on sulfided W^{4+} species remains practically constant for all catalyst formulations except for the pure titania supported catalyst in which its intensity substantially increases. Somewhat similarly, the area per square meter of catalyst of the band assigned to adsorbed NO on sulfided Ni^{2+} species increases slightly with titanium content up to the sample NiW/Al–Ti(0.95) and then sharply for the NiW/Al–Ti(1.0) sample. These results point out the existence of a higher density of NO adsorbing sites in the pure titania supported catalyst.

To obtain a more clear idea on the dispersion of the sulfided tungsten phases in the NiW/Al–Ti(x) catalysts, HREM observations were made for all the catalyst samples. As can be observed in Fig. 4, the micrograph shows the existence of the typical WS_2

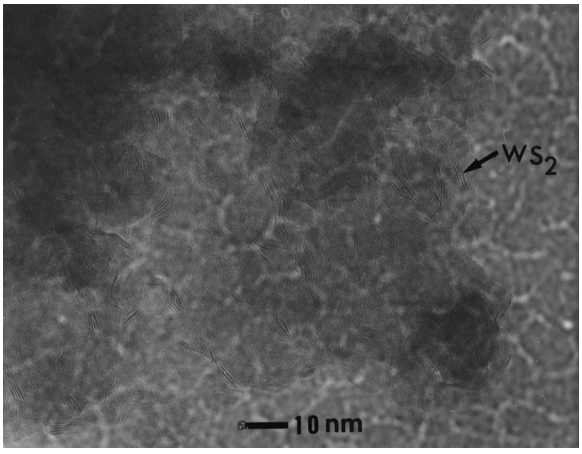

Fig. 4. HREM micrograph of NiW/Al–Ti(0.7) sulfided catalyst.

layered structures with interplanar distances of about 6.1 Å. The population and the length of these crystallites increased with the titanium content in the catalyst. Statistics over more than 500 crystallites per catalyst sample allowed a quantitative estimate of the average size and number of layers of the WS_2 crystallites in the different catalysts samples. In general, the results showed that the maximum of the size distribution plots for the alumina-rich samples (NiW/Al–Ti(0, 0.1)) was at 20–30 Å, for the NiW/Al–Ti(0.5, 0.7) samples at 30–40 Å, for the NiW/Al–Ti(0.95) sample at 40–50 Å, and for the pure titania supported sample, NiW/Al–Ti(1.0), at 20–30 Å. Apparently, the WS_2 crystallite size in the catalysts supported on Al–Ti mixed oxides (x=0.1 to x=0.95) increases with titanium content but for the catalyst supported on pure titania the size of the WS_2 crystallites diminishes again. Without considering this latter catalyst, the dispersion of WS_2 appears to diminish with the titanium content. However, one must bear in mind that the sulfidation of the alumina rich tungsten supported catalysts seems, according to the TPR results, very poor. Therefore in the titanium containing samples, the growing of the WS_2 crystallites might be the result of different levels of catalyst sulfidation. In other words, the observation of longer WS_2 crystallites is not due to a sintering process but rather to the fact that a major proportion of the tungsten oxidic species is being sulfided as the titanium content increases.

Regarding the stacking of the WS_2 crystallites, in all the catalyst samples the results indicate that most of the WS_2 crystallites were only one layer. However, the percentage of crystallites with greater number of layers decreased with the titanium content.

4. Discussion

According to our TPR results, the increase of titanium in the catalyst support leads to tungsten species with less interaction with the support which therefore reduce more easily than those supported on alumina. This improvement in reducibility may be due to the decrease of the interaction between the tungsten oxidic species and the support as the titanium loading is increased. In addition, effects due to the reducible behavior of TiO_2 and its semiconductor character may play a role considering that according to previous publications, TiO_2 has a conduction band very close to that of WO_3 [15]. The total hydrogen consumption and the degree of reducibility, estimated on the assumption that only the tungsten and nickel are reduced, show that the reducibility increases with the titanium content (See Table 3). However, this assumption is not completely accurate since part of the titania support is also reduced. It is for this reason that the degree of reducibility, estimated under the above assumption, reaches values beyond 120%. A more accurate estimation of the degree of reducibility of the tungsten and nickel species was not attempted since by this method it is not clearly known how much of the titania support is reduced. However, from the numbers in Table 3 it appears that only a few TiO_2 surface layers are reduced.

Comparison of the XPS experimental results in the form of atomic ratios with those predicted from the

Table 3
Calculated hydrogen consumption and degree of reducibility for the NiW/Al–Ti(x) catalysts

Catalyst	H_2 consumption ($mmol/m^2$)$\times 10^4$	[a] Degree of reducibility (%)
NiW/Al–Ti(0)	17.71	52.79
NiW/Al–Ti(0.1)	20.32	63.71
NiW/Al–Ti(0.5)	20.95	66.25
NiW/Al–Ti(0.7)	20.28	70.46
NiW/Al–Ti(0.95)	31.80	87.53
NiW/Al–Ti(1.0)	46.25	119.34

[a] Assuming that only nickel and tungsten are reduced.

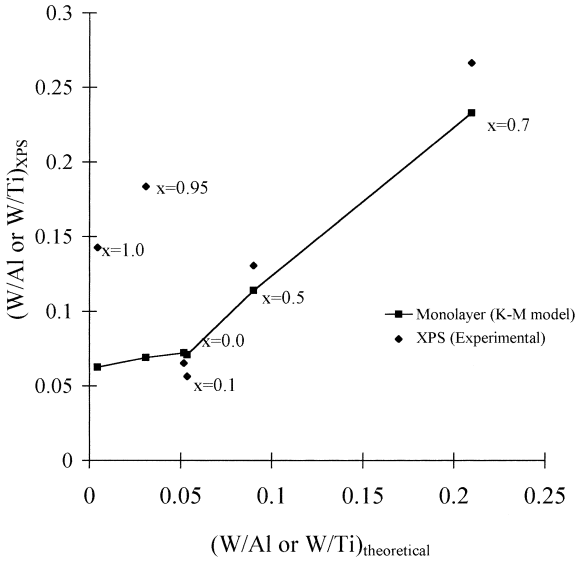

Fig. 5. Experimental (◆) and theoretical XPS W/Al or W/Ti atomic ratios (-■-) estimated assuming a monolayer coverage according to Kerkhof–Moulijn model.

Kerkhof–Moulijn (K–M) model [16–18] which assumes a monolayer coverage, may allow a better interpretation of the dispersion of tungsten on the different catalysts. However, in our case since the composition of the support changes from one formulation to another, it is difficult to plot for all the range of compositions the ratios of the atomic concentration of tungsten to the atomic concentration of the metal in the support (Al or Ti). Therefore, after trying different possibilities, we decided to divide the calculation in two regions. The samples from x=0 to x=0.5 were calculated considering that alumina was the main support and for the samples with x=0.7 to x=1.0, titania was considered as the main support. Fig. 5 shows the experimental W/Al and W/Ti atomic ratios (single points) compared to the estimated monolayer value calculated from the K–M model (solid line). The W/Al ratio for the NiW/Al–Ti(x=0, 0.1, 0.5) catalysts is fairly close to the monolayer value, therefore one can assume a good tungsten dispersion on these catalysts. However, as the titanium concentration is increased further (x=0.7), a surface enrichment of tungsten species is observed since the experimental value of the W/Ti ratio is higher than the one expected at monolayer coverage. This surface enrichment is even more notable for the NiW/Al–Ti(0.95, 1.0) samples. It appears that in the alumina-rich catalysts (x=0 to x=0.5) the tungsten species are highly dispersed possibly due to the strong interaction of the W species with the alumina-rich support, and that at high titania contents the interaction of the tungsten species with the support is diminished allowing the migration of tungsten species to the external surface. These observations are in agreement with the UV–VIS diffuse reflectance spectra of similarly prepared W/Al–Ti(x) catalysts which show a gradual increase in the octahedral tungsten species, which are more easily reduced than the tetrahedral ones, as the Ti content in the support increases [5]. For the Ni-promoted catalysts, the UV–VIS (DRS) results indicate that the ratio $Ni(O_h)/Ni(T_d)$ drops with the first additions of titania (x=0.1), and then begins to increase once the catalyst formulation goes beyond x=0.5. The decrease in catalytic activity observed for the NiW/Al–Ti(0.1) sample may well be related to the drop in the Ni(Oh)/Ni(Td) ratio. On the other hand, for the titanium-rich catalysts, the increase of the $Ni(O_h)/Ni(T_d)$ ratio might be related to the appearance of some highly dispersed particles of TiO_2 evidenced by the drop in the dispersion of Ti detected by XPS and by the detection, by XRD, of TiO_2 anatase particles (x=0.95, 1.0). As it is well known, TiO_2 has only octahedral coordination whereas in alumina both octahedral and tetrahedral coordination exist. Therefore, since the nickel is also interacting with the support, more octahedral Ni species are expected to the extent that more titania and less alumina is present on the catalyst surface. Indeed, the DRS results indicate a change in the distribution of Ni and W species with the incorporation of Ti to the support giving rise to an increase in the population of octahedral Ni and W species. However, since the DRS measurements were made at ambient conditions, it is quite likely that the coordination of some of the surface tungsten mono-oxo wolframyl species changes with the coordination of water leading to six-fold coordinated octahedral tungsten species. Nevertheless, it appears that the strength of the interaction of the tungsten species with the support decreases with titanium loading, rendering them more reducible. Also, the octahedral Ni species which increases with titania loading, are more reducible than those in tetrahedral coordination such as $NiAl_2O_4$ (6), the formation of which would be more likely in the alumina rich catalysts. It is because of the presence of

these more reducible species that the TPR results show an increase in the degree of reducibility of the NiW/Al–Ti(x) catalysts with the titanium content.

It also appears that not only does the titanium induce the presence of W species with less interaction with the support and more reducible, but also the incorporation of the Ni promoter induces a substantial change in the tungsten species. This is clearly observed when comparing the TPR traces of the Ni-promoted and unpromoted catalysts with x=0.5 (see Fig. 2(b) and (c)). In this figure, it is evident that the number of observed tungsten species is diminished and that the reduction temperatures are shifted to lower values when Ni is incorporated to the catalyst formulation. In the same figure, (Fig. 2(c)), the peak with T_{max}=883 K is assigned to the reduction of highly dispersed NiO species as well as to the same reduction of the TiO_2 on the support, as previously reported [5]. The changes induced by the support formulation on the catalyst oxidic precursors are also reflected in the characteristics of their sulfided state. As the catalyst titanium content is increased, the HREM observations and the NO adsorption results indicate that there is an increase in the population of W sulfided species and also an increase in the number of tungsten and nickel NO adsorbing sites. The HREM results also indicate that in the catalysts supported on Al–Ti mixed oxides there is a lateral growth of the WS_2 crystallites which does not appear to come from a sintering process but rather from a higher level of sulfidation of the tungsten oxidic species which, in the Al-rich catalysts, are in strong interaction with the support and hard to sulfide. To support this idea, an estimate of the number of WS_2 crystallites, observed in the micrographs in a given area, was obtained from the catalyst micrographs. Also, from the micrographs, it is possible to determine the average size (L) and number of layers (N) of the WS_2 crystallites and thus, estimate the number of observed sulfided tungsten atoms. Therefore, an estimation of the degree of sulfidation of each catalyst sample, expressed as the % of the tungsten sulfided atoms, can be made since we know the total tungsten atomic surface concentration of each catalyst (2.8 W atoms/nm^2). The results from this exercise, made assuming regular hexagonal shapes of the WS_2 crystallites as suggested by Kaztelan's geometrical model [18], show that the degree of sulfidation increases with titanium content but that it is only after the catalyst formulation is rich in titania ($x \geq 0.7$) that it is substantially increased. In fact, results from this calculation indicate that the catalysts with $x \leq 0.5$ are poorly sulfided whereas the titania rich catalysts (x=0.95, 1.0) are almost completely sulfided under the same conditions. As expected, the degree of sulfidation of the W species estimated in this way does not go beyond 100%, as it did the degree of reducibility estimated from TPR measurements, where also the Ni and part of the Ti species are reduced.

On further analysis of our results from the geometrical model of the WS_2 crystallites, it should be interesting to see if, for the 'well sulfided catalysts' (x=0.7, 0.95, 1.0), it is possible to relate the catalytic HDS activity to the population of edge or corner tungsten sites of the WS_2 crystallites present in each catalyst formulation. To this end, Fig. 6 presents the WS_2 crystallite model and the relationships used to estimate the number of tungsten atoms in each position.

Table 4 presents the values of the experimental reaction rates, average length and the number of layers of the WS_2 crystallites as well as the calculated

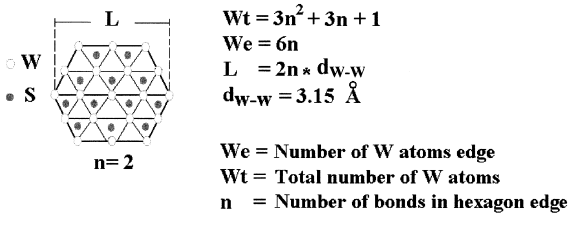

Fig. 6. WS_2 crystallite model and relationships used to estimate the number of tungsten atoms.

Table 4
Catalytic activity, HREM data, average length and average number of layers in WS_2 crystallites, and calculated parameters from Fig. 6

Sulfided catalyst	Ra (10^4)	L	N	a	a/N
NiW/Al–Ti(0)	7.79	37.28	1.66	0.29	0.17
NiW/Al–Ti(0.1)	4.48	35.34	1.40	0.30	0.21
NiW/Al–Ti(0.5)	6.51	37.37	1.60	0.29	0.18
NiW/Al–Ti(0.7)	8.98	39.31	2.53	0.27	0.11
NiW/Al–Ti(0.95)	17.30	51.13	1.50	0.22	0.15
NiW/Al–Ti(1.0)	32.40	35.75	1.28	0.30	0.23

Ra=thiophene molecules/tungsten atom-s; (L) average length and (N) number of layers of WS_2 crystallites; a (W edge/corner atoms)/(total W atoms).

fraction of edge or corner tungsten atoms per WS_2 crystallite (a) and per WS_2 crystallite layer (a/N).

Clearly, there is no correlation between the reaction rates and the total fraction of tungsten atoms at edge or corner positions (a). Since the main difference between samples in this analysis is the average number of layers of the WS_2 crystallites for each catalyst formulation, this result implies that under reaction conditions not all the layers of the WS_2 crystallites behave in the same way. We, therefore, attempted a correlation of the reaction rate with the fraction of tungsten atoms present in one layer of the crystallites (a/N). In other words, we considered that at a given time only the number of tungsten atoms equivalent to one layer was potentially active. This assumption was based on the consideration that once a thiophene molecule was adsorbed on one tungsten sulfur vacancy, those tungsten atoms, below or above the one where thiophene adsorption took place were sterically hindered from adsorbing another molecule of reactant.

The correlation between Ra and a/N, shown in Fig. 7, seems to be quite satisfactory. The fact that the straight line does not point to the origin only means that as the number of layers in the WS_2 crystallites increases the hexagonal form assumption of the WS_2 crystallites no longer holds since more agglomeration takes place.

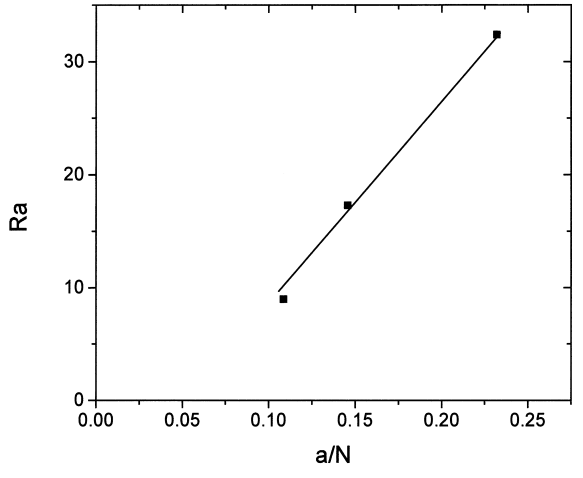

Fig. 7. Correlation between the thiophene HDS reaction rate, Ra, and the fraction of tungsten atoms at edge or corner positions per WS_2 layer, a/N.

5. Conclusions

From the above results the following conclusions can be drawn:

1. The incorporation of titania to the support in W and NiW/Al–Ti (x) catalysts increases the reducibility and sulfidability of the W species. The incorporation of the Ni promoter also enhances the reducibility of the tungsten species.
2. During the sulfidation process, a thin layer of the TiO_2 present in the support is also sulfided.
3. The XPS results indicate that for the titania-rich catalysts ($x \geq 0.7$), which show tungsten concentrations above the monolayer coverage estimated by the K–M model, there is an outer surface enrichment (near the pore mouths) of tungsten oxidic species which seems to be due to the diminished interaction between the tungsten oxidic phases and the support.
4. For the well sulfided NiW/Al–Ti(x) catalysts ($x > 0.7$), the catalytic activity in thiophene HDS correlates well with the number of tungsten atoms in edge and corner positions present in only one layer of the WS_2 crystallites. This can be rationalized by considering that, at a given time, during the adsorption of reactants on a given edge or corner tungsten atom, the tungsten atoms above and below the former, and located in different layers of the same WS_2 crystallite, are sterically hindered and therefore do not adsorb reactant molecules until all other tungsten atoms above and below the former are reactant-free.

Acknowledgements

We kindly acknowledge financial support from PEMEX-Refinación, IMP (FIES program), and DGAPA-UNAM.

References

[1] J. Ramírez, S. Fuentes, G. Díaz, M. Vrinat, M. Breysse, M. Lacroix, Appl. Catal. 52 (1989) 211.
[2] W. Zhaobin, X. Qin, G. Xiexinan, E.L. Sham, P. Grange, B. Delmon, Appl. Catal. 63 (1990) 305.
[3] M. Breysse et al., Catal. Today 4 (1988) 39.

[4] J. Grimblot, L. Gengembre, A.D′ Huysser, J. Elec. Spec. Rel. Phen. 52 (1990) 485.
[5] J. Ramírez, A. Gutiérrez-Alejandre, J. Catal. 170 (1997) 108.
[6] B. Scheffer, P. Molhock, J.A. Moulijn, Appl. Catal. 46 (1989) 11.
[7] D. Vermaire, P. vanBerge, J. Catal. 116 (1989) 309.
[8] G. Ramis, G. Busca, C. Cristiani, L. Lietti, P. Forzatti, F. Bregani, Langmuir 8 (1992) 1744.
[9] L. Salvati, L.E. Makovsky, J.M. Stencel, F.R. Brown, D.M. Hercules, J. Phys. Chem. 85 (1981) 3700.
[10] K.T. Ng, D.M. Hercules, J. Phys. Chem. 80 (1976) 2094.
[11] H. Windawi, F. Floyd, L. Ho, Applied Electron Spectroscopy for Chemical Analysis, Wiley-Interscience, New York, 63, 1982, p. 156.
[12] T. Halachev, P. Atanasova, Ch. L. Vladov, J.L. Fierro, A. López-Agudo, Bull. Soc. Chim. Belg (1995).
[13] A. Benítez-Patricio, Ph.D. Thesis, Universidad Complutense, Madrid Espana, 1992, pp. 160–165.
[14] J.C. Lavalley, F. Mauge, D. Ouafi, Bull. Soc. Chim. France 3 (1989) 363–369.
[15] M.C. Paganini, L. Dall Acqua, E. Giamello, L. Lietti, P. Forzatti, G. Busca, J. Catal. 166 (1997) 195.
[16] F.P.J.M. Kerkhof, J.A. Moulijn, J. Phys. Chem. 83 (1979) 1612.
[17] V. León, A Simplified Kherkof–Moulijn Model for Dispersion Quantification from XPS Atomic Concentrations, INTEVEP, S.A..
[18] S. Kasztelan, H. Toulhoat, J. Grimblot, J.P. Bonnelle, Appl. Catal. 13 (1984) 127.